Environmental Science & Technology

pubs.acs.org/est

Article

Thermal Decomposition of Two Gaseous Perfluorocarboxylic Acids: Products and Mechanisms

Junli Wang, Mingrui Song, Ibrahim Abusallout, and David Hanigan*

Cite This: *Environ. Sci. Technol.* 2023, 57, 6179−6187

Read Online

ACCESS | Metrics & More | Article Recommendations | Supporting Information

ABSTRACT: The thermal decomposition products and mechanisms of per- and polyfluoroalkyl substances (PFASs) are poorly understood despite the use of thermal treatment to remediate PFAS-contaminated media. To identify the thermal decomposition products and mechanisms of perfluorocarboxylic acids (PFCAs), gaseous perfluoropropionic acid (PFPrA) and perfluorobutyric acid (PFBA) were decomposed in nitrogen and oxygen at temperatures from 200 to 780 °C. In nitrogen (i.e., pyrolysis), the primary products of PFPrA were $CF_2{=}CF_2$, CF_3CF_2H, and CF_3COF. $CF_3CF{=}CF_2$ was the dominant product of PFBA. These products are produced by HF elimination (detected as low as 200 °C). CF_4 and C_2F_6 were observed from both PFCAs, suggesting formation of perfluorocarbon radical intermediates. Pyrolysis products were highly thermally stable, resulting in poor defluorination. In oxygen (i.e., combustion), the primary product of both PFPrA and PFBA below 400 °C was COF_2, but the primary product was SiF_4 above 600 °C due to reactions with the quartz reactor. Oxygen facilitated thermal defluorination by reacting with PFCAs and with pyrolysis products (i.e., fluoroolefins and fluorocarbon radicals). Platinum improved combustion of PFCAs to COF_2 at temperatures as low as 200 °C, while quartz promoted the combustion of PFCAs into SiF_4 at higher temperatures (>600 °C), highlighting the importance of surface reactions that are not typically incorporated into computational approaches.

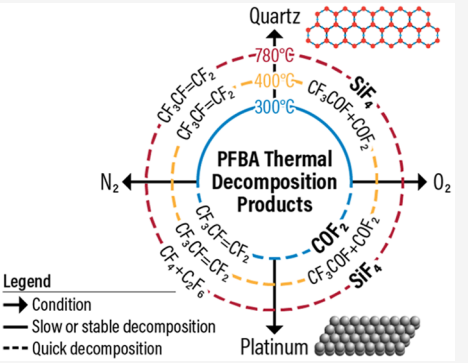

KEYWORDS: *PFCAs, pyrolysis, combustion, PFAS, thermal treatment*

1. INTRODUCTION

Per- and polyfluoroalkyl substances (PFASs) are fluorinated organic chemicals used in numerous products such as cosmetics,[1,2] nonstick coatings, packaging, pesticides, and aqueous film-forming foams.[3] The widespread use of PFASs and their long half-lives in the environment have led to their detection in water, soil, and air.[4−9] Human exposure to PFASs is associated with multiple negative health outcomes, including cancer, decreased birth weight, and immune system and lipid metabolism disruption.[3,10] Similar ecological health outcomes have also been observed for animals exposed to PFASs, in part because some PFASs are highly bioaccumulative.[11,12] The toxicity, bioaccumulation, and persistence of PFASs have attracted the attention of the scientific and regulatory community.[13]

To address PFAS contamination, thermal treatments such as incineration,[14−16] smoldering,[17] pyrolysis of biosolids,[18,19] and regeneration of granular activated carbon (GAC)[20−22] are currently being studied. There is a substantial body of research focusing on computational predictions of perfluorocarboxylic acids (PFCAs) decomposition based on density functional theory (DFT). Results from these studies have suggested that the primary pyrolysis mechanism of perfluoropropionic acid (PFPrA),[23] perfluorobutyric acid (PFBA),[24] and perfluoropentanoic acid[25,26] is HF elimination via reaction 1, yielding perfluoroacyl fluoride. Reactions 2 and 3 have been proposed to be minor pathways. However, when perfluorooctanoic acid (PFOA) was experimentally evaluated in a quartz or aluminum reactor, there was a divergence between the DFT-proposed and experimental products; only reactions 2 and 3 were observed.[27,28] Additionally, DFT models do not typically capture the surface effects of reactor materials or catalysts, highlighting the need for experimental verification of thermal decomposition mechanisms and products.

$$C_nF_{2n+1}COOH \rightarrow C_{n-1}F_{2n-1}COF + HF + CO \quad (1)$$

$$C_nF_{2n+1}COOH \rightarrow C_{n-2}F_{2n-3}CF{=}CF_2 + HF + CO \quad (2)$$

$$C_nF_{2n+1}COOH \rightarrow C_{n-1}F_{2n-1}CF_2H + CO_2 \quad (3)$$

Published experimental research has focused on the temperature required to decompose PFCAs, rather than the mechanisms, and has demonstrated that decomposition begins at ∼200 °C and partial mineralization (>86%) occurs above

Received: November 4, 2022
Revised: February 24, 2023
Accepted: March 21, 2023
Published: April 5, 2023

https://doi.org/10.1021/acs.est.2c08210
Environ. Sci. Technol. 2023, 57, 6179−6187

700 °C.[21,29−32] With addition of calcium hydroxide or calcium oxide above 400 °C, fluorine from perfluorooctanesulfonic acid (PFOS) (>60%) and PTFE (>80%) was mineralized and fixed as calcium fluoride.[15,33] When PFASs were sorbed to GAC prior to thermal treatment, the temperature required to initialize decomposition of PFASs was substantially lower than the temperature of those not sorbed to GAC. This was attributed to a catalytic effect of the relatively mobile electrons in the GAC surface,[22] but overall, surface effects and catalysis of PFAS thermal decomposition have been relatively poorly studied.

Volatile organofluorine (VOF) can also be formed during the thermal decomposition of PFASs[21,34] and can be transported long distances (>150 km),[35] but the formation and fate of volatile decomposition products are not well understood. Mass balances on fluorine during thermal treatment are rarely achieved,[19] and low mineralization rates of fluorine indicate the formation of organofluorine and/or VOF.[20,34] For example, the VOF yield was as high as 13% during thermal treatment of GAC loaded with PFOA[34] and VOF such as CF_4 and C_2F_6 are extremely challenging to thermally decompose, even up to 1000 °C.[36] Thus, it is imperative to understand the formation of VOF during thermal treatment to identify treatment alternatives that mitigate VOF release.

Finally, both combustion (in oxygen) and pyrolysis (in an inert atmosphere) are parts of thermal treatment.[18,31] It is known that O_2 improves mineralization of PFASs, but the mechanisms are again not well understood.[36,37] The objectives of this study were (1) to compare the decomposition pathways proposed by computational studies to experimental results, (2) to understand the effects of temperature on thermal decomposition and/or mineralization of PFCAs and respective VOF formation, (3) to identify the role of O_2 in the thermal mineralization of PFCAs, and (4) to assess the effect of reactor materials, including quartz (present in nearly all previous studies of PFAS decomposition as the reactor material) and platinum (Pt), on decomposition. To achieve these goals, we investigated the fate and transformations of two model PFCAs, PFPrA and PFBA, in nitrogen (N_2) and O_2 atmospheres at temperatures from 200 to 780 °C via Fourier transform infrared spectroscopy (FTIR). PFPrA and PFBA were selected because they were volatile enough in initial experiments to produce a FTIR signal when the headspace gas above a neat standard was introduced into the FTIR cell and because the decomposition mechanisms are likely to be similar for all PFCAs, a commonly observed group of PFASs in the environment.

2. MATERIALS AND METHODS

2.1. Reagents and Materials. PFPrA and PFBA (both in their acid forms) and 350 mg of Pt foil (0.025 mm thickness, 99.9%) were purchased from Sigma-Aldrich (St. Louis, MO). Quartz wool was purchased from COSA Xentaur (Houston, TX). Two Pt wires (0.25 mm diameter, 100 cm length) were purchased from Alfa Aesar (Tewksbury, MA).

2.2. Thermal Decomposition Experiments. A modified Shimadzu TOC-VCSH instrument was used as a temperature-controlled furnace for the thermal treatment of PFCAs.[32] The temperature was controlled through the instrument software. A quartz combustion tube was packed with 0.3 g of quartz wool to prevent short circuiting in the combustion tube or Pt wire and foil to test the potential for catalytic degradation.[32] O_2 or N_2 carrier gases were passed through the combustion tube at a rate of 300 mL/min. A stoppered vial containing <1 mL of pure PFPrA or PFBA was connected in parallel with the carrier gas line. The combustion tube was interfaced to a 5 m optical path FTIR gas cell. The gas downstream of the combustion module was monitored by a Shimadzu IRTracer-100 instrument equipped with a MCT (mercury−cadmium−telluride) detector. The resolution of FTIR was 2 cm^{-1}. The number of scans to produce a spectrum was three, taking 12 s to acquire.

Each thermal decomposition experiment was conducted under four variable conditions: reactants (PFPrA and/or PFBA), temperature (200−780 °C), atmosphere (N_2 or O_2), and packing material (quartz wool and/or Pt). Before each experiment, the stoppered vial and gas cell were purged with carrier gas at a flow rate of 300 mL/min to remove interference from air. Initially, the carrier gas bypassed the stoppered vial and flowed directly into the combustion tube (Figure 1), and

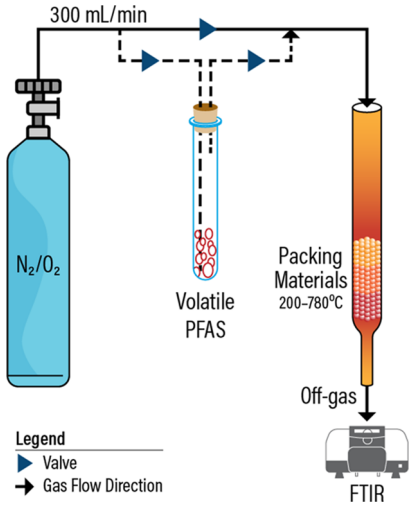

Figure 1. Schematic of the experimental approach.

the temperature of the combustion tube was set to 200 °C. When the temperature of the combustion tube and the FTIR baseline were stable, the headspace gas from the stoppered vial containing either PFPrA or PFBA was introduced by altering the carrier gas flow path. For 3 s (PFPrA) or 10 s (PFBA), to produce a sufficiently strong FTIR signal to interpret the spectra without saturating the detector (based on initial experiments), the carrier gas flowed through the headspace of the stoppered vial. PFBA required more time because of the lower vapor pressure.[38] The carrier gas flow path was then returned to directly flow to the combustion tube. The FTIR spectra were scanned and recorded every 1 min for the first 4 min and then every 2−3 min later until no signal remained, approximately 20 min later. The temperature was then adjusted as needed (e.g., 300, 400, 600, and 780 °C), and the FTIR baseline was reset. Spectra with the strongest peaks but having an intensity of <1 absorbance unit were utilized for product identification, and IR peak assignments are listed in Table S1.

2.3. Product Identification Approach. Products were identified by matching observed FTIR spectra with published spectra from the NIST Chemistry Webbook,[39] spectrabase.com,[40] or journal publications.[41−48] Reference spectra and the spectra from this study are listed in Table S1. For the sake of clarity during comparisons, reference spectra were adjusted by

https://doi.org/10.1021/acs.est.2c08210
Environ. Sci. Technol. 2023, 57, 6179−6187

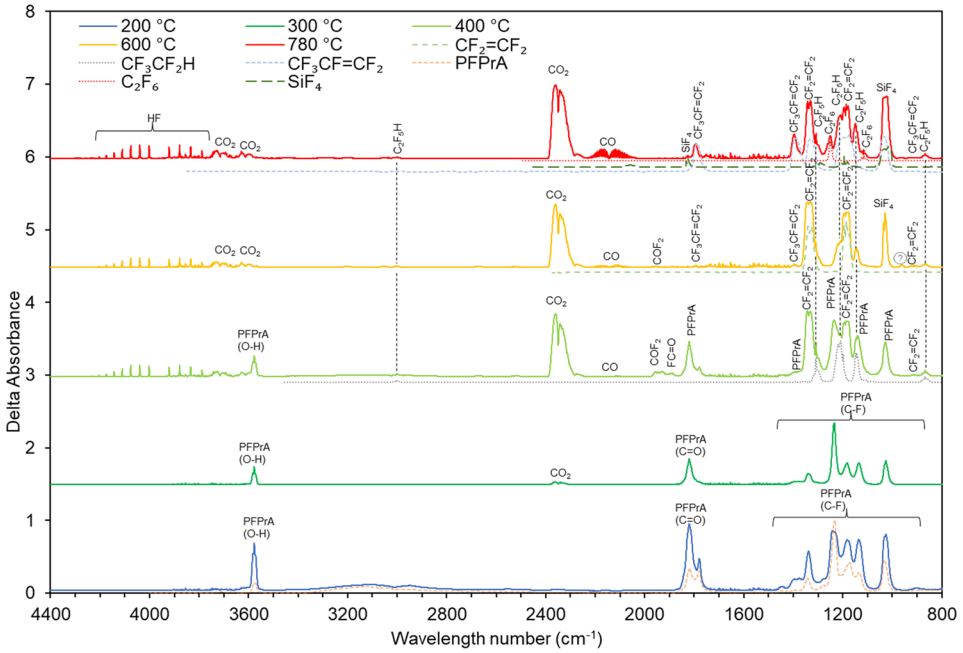

Figure 2. Infrared spectra acquired during pyrolysis of PFPrA in N_2 at temperatures from 200 to 780 °C. Dashed and dotted lines are standard spectra from the library (see Table S1).

multiplying by a constant. The spectra of organofluorine compounds, including PFPrA, PFBA, 1*H*-perfluoroethane (CF_3CF_2H), CF_2═CF_2, CF_3CF═CF_2, COF_2, CF_3COF, and C_2F_6, were in some cases partially obscured due to overlapping peaks of other products. When partial overlap occurred, products were confirmed by two additional characteristic peaks that were not obscured by other products in the fingerprint region. Spectra of inorganic species, including CO_2, CO, HF, and SiF_4, rarely overlapped with those of other products. In one case, the SiF_4 peak at 1030 cm^{-1} during the pyrolysis of PFBA above 600 °C was completely obscured by CF_3CF═CF_2. However, the spectra of SiF_4 could be clearly observed at two adjacent temperatures, 600 and 780 °C, where the spectrum of CF_3CF═CF_2 was weaker (Figure S5). Each of the identified products was observed at least twice in separate experiments.

To describe the relative absorbance intensity of the formed products in Figures 3 and 4, we defined four terms: dominant, strong, intermediate, and weak. We define "dominant" as a peak or group of related fluorine-containing peaks from the reagent (e.g., parent PFAS) or decomposition products that were most prevalent in the spectra. In many cases, a dominant product was the only peak or set of associated peaks in the spectra (see Figure S1B at 600 °C, where C_3F_6 is the dominant peak). "Strong" was a product with a peak absorbance of >0.3. "Intermediate" was a product with an absorbance between 0.1 and 0.3. "Weak" had an absorbance of <0.1. We have included these groupings to relate the relative intensity of the products in a succinct way, and the full spectra are provided in the Supporting Information.

3. RESULTS AND DISCUSSION

3.1. Pyrolysis of PFCAs. *3.1.1. Pyrolysis in the Presence of Quartz.* PFPrA and PFBA were pyrolyzed between 200 and 780 °C in a quartz reactor partially filled with quartz wool to impede short circuiting. An example FTIR spectrum during PFPrA pyrolysis is shown in Figure 2, and a summary of the products of both PFPrA (CF_3CF_2COOH) and PFBA ($CF_3CF_2CF_2COOH$) is shown in Figure 3. The products fell

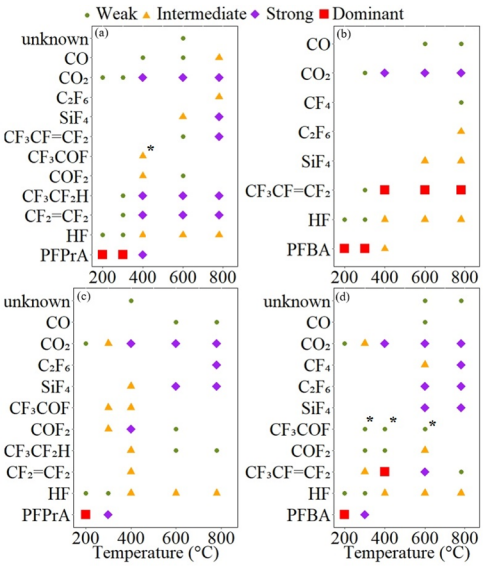

Figure 3. Pyrolysis products in N_2 at various temperatures: (a) PFPrA (b) PFBA, (c) PFPrA with Pt, and (d) PFBA with Pt. FTIR spectra are provided in Figures S1 and S2. Weak, intermediate, strong, and dominant are defined in Materials and Methods. An asterisk indicates that only the COF group was confirmed.

into three categories: inorganic fluorine (i.e., HF and SiF_4), identified and unidentified organofluorine, and mineralized carbon (i.e., CO and CO_2). At 200 °C, organofluorine products were not observed for either PFPrA or PFBA. HF was, however, observed at 200 °C (Figure S6), suggesting that the decomposition of PFPrA and PFBA by HF elimination is initiated at relatively low temperatures. Beginning at 300 °C, olefins were present (Figure S7), and at ≥400 °C, most or all

https://doi.org/10.1021/acs.est.2c08210
Environ. Sci. Technol. 2023, 57, 6179−6187

of reactants were decomposed to their respective olefins (i.e., PFPrA → CF_2=CF_2; PFBA → CF_3CF=CF_2) and CF_3CF_2H (only from PFPrA). Above 600 °C, SiF_4 and C_2F_6 were also formed from both PFPrA and PFBA.

Prior computational studies have suggested that reaction 1 dominates pyrolysis of PFCAs,[23,24,26] but during pyrolysis of PFBA, the corresponding CF_3CF_2COF was not detected at any temperature. For PFPrA at 400 °C, we observed C=O stretching at 1898 cm^{-1}, which can be attributed to the acyl fluoride group (-COF) in CF_3COF[45] as predicted by reaction 1 (Figure 2). However, other computational and experimental research has suggested that the observed acyl fluoride functional group may also be formed during the pyrolysis of PFASs via reactions with HF (reaction 4), forming a corresponding CF_3CF_2COF from PFPrA rather than CF_3COF (reaction 1).[25,49] The -COF peak was relatively small, and C−F stretching was somewhat obscured by other products. However, considering that some HF formation was concurrently present in the spectra and that some COF_2 was also concurrently observed (likely formed via reaction 5, which requires CF_3CF_2COF),[50,51] the -COF peak is likely associated with CF_3CF_2COF. Overall, we find that reaction 1 is unlikely to play a major role in the pyrolysis of PFCAs below ∼600 °C in a quartz reactor. This is further supported by the lack of observed $C_6F_{13}COF$ being formed via reaction 1 during PFOA pyrolysis in two other publications.[27,28]

$$CF_3CF_2COOH + HF \rightarrow CF_3CF_2COF + H_2O \quad (4)$$

$$CF_3CF_2COF \rightarrow CF_2{=}CF_2 + COF_2 \quad (5)$$

Reactions 2 and 3 have been proposed to be minor pathways by a computational study,[23] but here we note that these pathways appear to be principal below ∼780 °C. The primary products of PFPrA pyrolysis were HF, CO_2, CF_2=CF_2, and CF_3CF_2H above 200 °C. These products are explained well by HF elimination via reactions 2 and 3. However, for PFBA, $CF_3CF_2CF_2H$ was not observed at any temperature, and therefore, reaction 3 does not appear to play a major role. Instead, CF_3CF=CF_2 was the dominant product at all temperatures, suggesting the dominant decomposition pathway is reaction 2. In another publication, the pyrolysis of PFBA sodium and potassium salts (e.g., $CF_3CF_2CF_2COONa$ and $CF_3CF_2CF_2COOK$, respectively) yielded >97% CF_3CF=CF_2,[52] agreeing well with our findings using protonated PFBA. PFBA has only one additional fluorinated carbon (CF_2) compared to PFPrA, but the decomposition products are substantially different, highlighting that for these two small molecules, small changes to the molecular structure can have large impacts on outcomes. Although these changes are substantial, we expect that for longer chain PFCAs the primary decomposition pathways will be among the three pathways identified here (reactions 1−3).

Above ∼600 °C, there appeared to be a substantial change in mechanism. For example, CF_3CF=CF_2 was formed at ≥600 °C during the pyrolysis of PFPrA, likely from the thermal transformation of CF_2=CF_2, which was also observed at ≥400 °C.[53,54] This transformation became more apparent at higher temperatures (Figure 2). It is well documented that CF_2=CF_2 is highly reactive, and some of the reactions can produce other VOF, including perfluorocyclobutane (cyclo-C_4F_8), perfluoroisobutene [$(CF_3)_2C$=CF_2], perfluoroethane (C_2F_6), and tetrafluoromethane (CF_4), although these products were not apparent in this study.[53,54]

Above ∼600 °C, CO and SiF_4 were also significant products. The reaction between HF and quartz forming SiF_4 is well-known, but HF is unlikely to be the primary source of SiF_4 because the system is hydrogen limited. It is more likely that CO and SiF_4 were formed from reactions between perfluorocarbon radicals and quartz, as reported by others.[55,56] The formation of C_2F_6 and CF_4 at 780 °C from both PFPrA and PFBA (Figure S1) also suggests the formation of perfluorocarbon radicals from homolysis of C−C and C−F bonds, which then terminate in these more stable molecules.

It is worth noting that the source of oxygen in CO and CO_2 not only is from the carboxyl group by reactions 1−3 but also may be from quartz (SiO_2) by reaction with fluorocarbon radicals.[55−57] CO_2 can also be formed during the pyrolysis of fluorocarbons (e.g., CHF_3 and C_4F_{10}) without supplemental oxygen in an aluminum reactor, and the oxygen was thought to be from aluminum.[58,59]

In summary, temperature is critical and delineates PFCA decomposition into two regions during pyrolysis. (1) From ∼200 to ∼600 °C, PFCA decomposition begins at the least stable functional group, the carboxylic acid, via HF elimination forming more stable fluorinated olefins and 1*H*-perfluoroalkanes. (2) Above ∼600 °C, perfluorocarbon radicals are produced, resulting in the formation of CF_4 and C_2F_6. Perfluorocarbon radicals also reacted rapidly with the quartz reactor, resulting in the formation of SiF_4. The reaction between radicals and the quartz reactor has implications for thermal treatment, where co-occurring waste materials may substantially alter the products from those that would be expected from computational analysis alone.

3.1.2. Catalyzed Pyrolysis with Pt. To understand the potential of surface effects to change the decomposition mechanisms, the quartz reactor was filled with large-surface area Pt foil and wire. The products of PFPrA and PFBA decomposition are shown in panels c and d of Figure 3, respectively. At 200 °C, the product spectra were similar to those produced without Pt; most reactants were not decomposed. The greatest difference between quartz and Pt packing was the disappearance of olefins at increased temperatures for both PFPrA and PFBA. For example, for PFPrA, CF_2=CF_2 was not observed above 400 °C with Pt but was present even at 780 °C when no Pt was present. For PFBA, CF_3CF=CF_2 was again present below 400 °C, but its level decreased with an increase in temperature, despite being the dominant product at all temperatures without Pt. For both PFPrA and PFBA, oxygen-containing products (e.g., COF_2 and CF_3COF) were formed to a greater extent in the presence of Pt, likely due to oxidation of the respective olefins by surface-bound reactive oxygen species[60−63] present from residual O_2 and H_2O sorbed when the Pt was not in use and exposed to air. CF_3CF_2H was also formed to a lesser extent from PFPrA in the presence of Pt compared to without Pt, although the difference in mechanism is not clear.

At 780 °C, C_2F_6 and CF_4 were formed to a greater extent in the presence of Pt, especially for PFBA (Figure S2). Formation of these two products over the olefin (CF_3CF=CF_2, when only quartz was present) indicates that perfluorocarbon radicals formed to a greater extent on the Pt surface than when no Pt was present. This is because the formation of C_2F_6 and CF_4 is primarily from reactions between perfluorocarbon radicals (i.e., radical termination).[59,64]

The signal associated with the -COF group observed during the pyrolysis of PFPrA without Pt was again observed with Pt,

https://doi.org/10.1021/acs.est.2c08210
Environ. Sci. Technol. 2023, 57, 6179−6187

and now the CF_3COF could clearly be identified from observed C−F stretching at 300 and 400 °C (Figure S2a). This suggests that although reaction 1 played a minor role without Pt, it was more important when Pt is present and indicates that surface effects can alter the decomposition pathways. This was particularly evident at 300 °C, where CF_3COF was a principal product, and little or no CF_3CF_2H or $CF_2{=}CF_2$ was present (Figure S2b), despite being formed when Pt was not present in the reactor (Figure 3c). Given that reaction 1 appears to be occurring with Pt, we also expected to find the product CO. However, no CO was observed. This is likely because CO was catalytically oxidized to CO_2 by oxygen or hydroxyl present on the Pt surface.[65] How Pt promotes reaction 1 is not clear, but it is apparent that the addition of Pt to the reaction mixture substantially changed the decomposition mechanisms of PFPrA.

For PFBA, the characteristic -COF peak at 1898 cm^{-1} was observed but it is not clear if it was from CF_3CF_2COF, which would be expected on the basis of the findings from PFPrA, due to multiple overlapping signals in the C−F region. COF_2 was also present simultaneously (Figure S2b), and therefore, this signal is more likely attributed to CF_3COF from the oxidation of $CF_3CF{=}CF_2$ on the surface of Pt by reaction 6.

3.2. Combustion of PFCAs. *3.2.1. Combustion with Quartz Wool.* Combustion (i.e., in the presence of O_2) products of PFPrA and PFBA with a quartz reactor and quartz packing are shown in panels a and b of Figure 4, respectively.

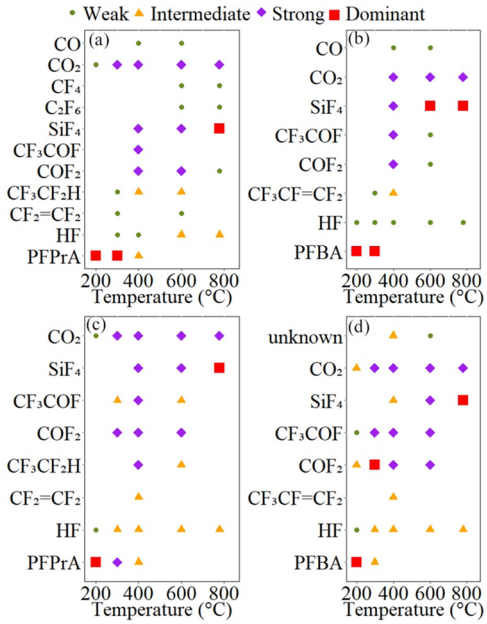

Figure 4. Combustion products in O_2: (a) PFPrA, (b) PFBA, (c) PFPrA with Pt, and (d) PFBA with Pt. The FTIR spectra are provided in Figures S3 and S4. Weak, intermediate, strong, and dominant are defined in Materials and Methods.

At 200 and 300 °C, O_2 did not substantially participate in the decomposition of PFPrA and PFBA; the products were similar to or the same as those produced by pyrolysis. One notable difference at 200 °C was that HF was formed less than by pyrolysis based on signal intensity, or not formed at all (Figure S6). It is not clear why HF was formed to a lesser extent.

At 400 °C, the extent of formation of CF_3CF_2H and $CF_2{=}CF_2$ from PFPrA was substantially reduced compared to that of pyrolysis (Figures S1a and S3a), but the production of COF_2 increased, based on the absorbance ratio of CF_3CF_2H or $CF_2{=}CF_2$ to COF_2. This may be because O_2 reacts with the olefin $CF_2{=}CF_2$, resulting in the formation of COF_2 via reaction 7, where $CF_2{=}CF_2$ was produced from PFPrA by reaction 2. When PFBA was combusted at 400 °C, CF_3COF and COF_2 were formed to a greater extent than during pyrolysis, and the extent of formation of the product $CF_3CF{=}CF_2$ was reduced (Figures S1b and S3b). This is explained well by reaction 6, and thus, it is likely that the observed COF_2 produced by PFPrA is produced through a similar reaction with the intermediate olefin (reaction 6), rather than direct reactions between PFPrA and O_2.

$$CF_3CF{=}CF_2 + O_2 \rightarrow CF_3COF + COF_2 \quad (6)$$

$$CF_2{=}CF_2 + O_2 \rightarrow 2COF_2 \quad (7)$$

We expected similar mechanisms at higher temperatures (i.e., O_2 oxidizes products formed through pyrolytic mechanisms, such as olefins into CF_3COF and COF_2) because during pyrolysis the mechanisms, involving the production of olefins, were similar at all temperatures (Figure 3). However, the dominant fluorinated product was SiF_4 for both PFPrA and PFBA above 600 °C (Figure 4). During pyrolysis, SiF_4 was a product of reactions between perfluorocarbon radicals and quartz, and most organofluorine products persisted up to 780 °C. However, with O_2 present at the same temperature, no organofluorine was observed in the gas phase from PFBA, and the majority of organofluorine was also mineralized for PFPrA. The complete mineralization of PFCAs to SiF_4 at these high temperatures makes it difficult to explain the mechanisms due to the lack of observed intermediates, which likely have extremely short half-lives and react with quartz or terminate through reactions with other radicals. PFPrA and PFBA likely form some intermediates produced through reactions with O_2 (possibly oxygen-containing fluorocarbon radicals), and these intermediates then preferentially react with quartz to form SiF_4. These reactions would also compete with perfluorocarbon radical recombination, explaining the lack of observable C_2F_6 and CF_4.

Overall, there was some overlap between the pyrolysis and combustion mechanisms. Below 300 °C, O_2 played a negligible role in thermal decomposition; between 400 and 600 °C, O_2 reacted with pyrolysis products (i.e., olefins), and above 600 °C, SiF_4 was the dominant product. We believe these two PFCAs yielded unidentified fluorocarbon radical intermediates through reactions with O_2, which then preferentially reacted with the quartz reactor to form SiF_4 as primary products. This, in turn, suppresses the formation of VOF (i.e., CF_4 and C_2F_6), which is difficult to destroy, and has implications for thermal treatment processes operating with excess oxygen, which may help to control VOF emissions at high temperatures.

3.2.2. Catalyzed Combustion with Pt. When Pt was introduced with O_2, the products of PFPrA were similar at 200 °C (Figure 4c) to those when only quartz was present. One important difference was that some PFBA was oxidized to COF_2 at 200 °C, and this did not appear to occur at this temperature without Pt (Figure 4b,d). At an only slightly higher temperature (300 °C), COF_2 was the primary product for both PFPrA and PFBA. Notably, when Pt was present, COF_2 did appear to originate from not only the oxidation of olefins but also the direct oxidation of PFCAs at or below 300 °C. We base this on the following. (1) Olefins were not

https://doi.org/10.1021/acs.est.2c08210
Environ. Sci. Technol. 2023, 57, 6179−6187

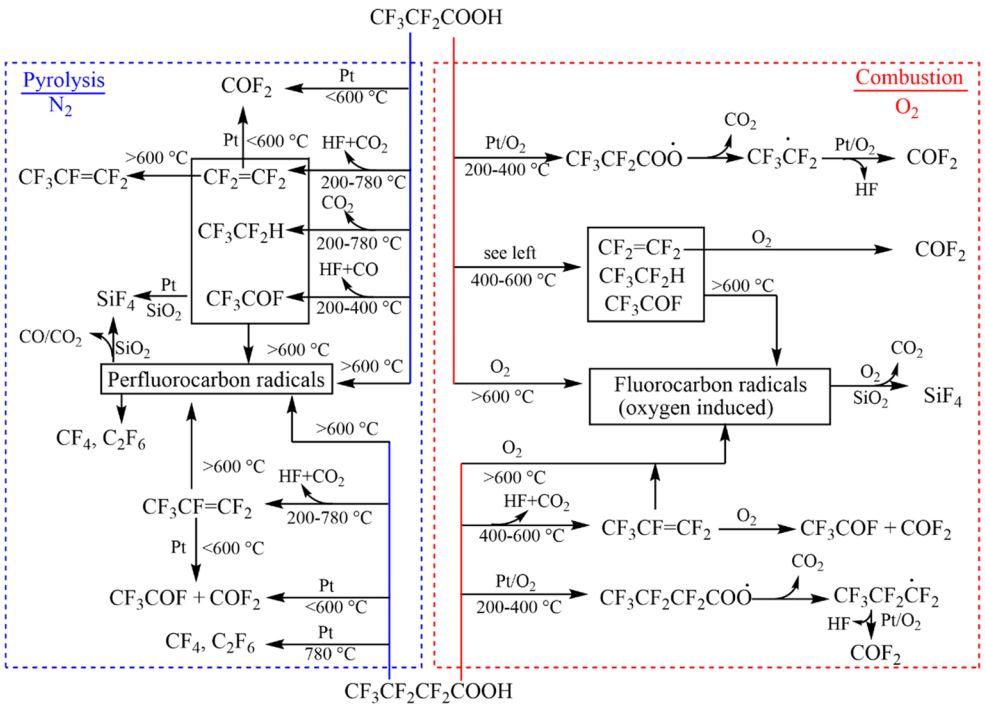

Figure 5. Proposed decomposition pathways of PFPrA (top) and PFBA (bottom) in the presence of quartz (SiO_2, reactor material) or Pt and quartz. Note that Pt can provide •OH/•O through reactions with surface-sorbed O_2 and H_2O. The combustion intermediates "fluorocarbon radicals" were not directly observed but are proposed on the basis of the products.

observed, and therefore, there is little or no olefin present to be oxidized to COF_2. (2) If the expected olefin $CF_3CF{=}CF_2$ was to be oxidized by O_2, it would result in COF_2 and CF_3COF absorbance spectra of similar intensity, similar to those at 400 and 600 °C shown in Figure S4b and reaction 7, but the COF_2 signal intensity was substantially greater than that of CF_3COF below 300 °C. Using DFT, Altarawneh et al. reported that the abstraction of hydrogen from the carboxylic acid group by •OH (reactions 8 and 9) yields $CF_3CF_2CF_2$•, which has the lowest activation energy of the abstractable sites.[66] $CF_3CF_2CF_2$• can then react with O_2 and •OH to form COF_2 (reactions 10 and 11),[67] facilitated by •OH present on the surface of Pt as a result of splitting of residual water and/or O_2.[60,62,63] These catalyzed thermal decomposition pathways were also derived on the basis of the results from other processes (i.e., photolysis, electrochemistry, and advanced oxidation) and have been compiled in a recently published review.[67] Below ∼300 °C, it appears that this pathway is dominant when Pt is present.

$$CF_3CF_2CF_2COOH + \bullet OH \rightarrow CF_3CF_2CF_2COO\bullet + H_2O \quad (8)$$

$$CF_3CF_2CF_2COO\bullet \rightarrow CF_3CF_2CF_2\bullet + CO_2 \quad (9)$$

$$CF_3CF_2CF_2\bullet + \bullet OH/O_2 \rightarrow 2COF_2 + CF_3\bullet \quad (10)$$

$$CF_3\bullet + \bullet OH \rightarrow 2COF_2 + HF \quad (11)$$

Between 400 and 600 °C, reactions 8−11, yielding COF_2, were less dominant. Instead, for both PFPrA and PFBA, unimolecular decomposition yielding olefins and 1*H*-perfluoroalkanes dominated, similar to pyrolysis. The intermediate olefins appeared to be terminally oxidized by O_2 to COF_2 and/or CF_3COF. Above 600 °C, mineralized products tended to dominate, including CO_2, HF, and SiF_4. CF_3COF and COF_2, which were the primary oxidized products at lower temperatures when Pt was present, were surprisingly not present at 780 °C. It is possible that at higher temperatures, PFPrA and PFBA were decomposed and formed SiF_4 in the top of a quartz tube via the perfluorocarbon radical pathway (section 3.2.1), before reaching the Pt placed in the lower portion of the tube, explaining why the products are the same as those from combustion with quartz.

3.3. Summary of Decomposition Pathways.

A summary of the primary observed decomposition pathways of PFPrA and PFBA is illustrated in Figure 5 on the basis of discussions presented above. It should be noted that the temperatures labeled in Figure 5 do not indicate a cutoff of decomposition mechanisms. Those decomposition pathways are likely to happen at all temperatures with varying kinetics, and the representation presented here embodies only the decomposition pathways that tend to outcompete other pathways in the labeled temperature ranges. The primary pyrolysis products, olefins and CF_3CF_2H, are highly stable up to 780 °C but readily react with O_2. In an inert atmosphere, Pt facilitated the decomposition of PFPrA and PFBA, and their pyrolysis products, although these mechanisms appeared to rely on surface-sorbed oxygen and thus are not truly pyrolysis. With O_2, Pt catalyzed the oxidation of PFBA at temperatures as low as 200 °C. Above 600 °C, quartz and O_2 together promoted the mineralization of PFCAs into SiF_4.

4. IMPLICATIONS

Thermal treatment presents an opportunity to end the PFAS cycle by mineralization to fluoride and carbon dioxide, but the mechanisms and thus potential to produce gaseous organofluorine products are not well understood. We show here that temperatures of <780 °C or the absence of oxygen results in relatively recalcitrant gaseous PFAS (e.g., olefins, CF_4, and

https://doi.org/10.1021/acs.est.2c08210
Environ. Sci. Technol. 2023, 57, 6179−6187

C_2F_6) from two PFCAs. Without further treatment of the off-gas, PFASs may be transferred from contaminated media to the atmosphere. Relevant systems include thermal desorption,[51,68,69] PFAS-laden GAC regeneration,[20,21,30,34] pyrolysis of biosolids,[18,19] and systems with slow heat or flame propagation. Post-treatment of produced gases during such treatment is likely to require additional high-temperature treatment (>780 °C) in the presence of excess O_2. In addition, combustion is usually conducted in an air (21% O_2) atmosphere, which may influence the efficiency of mineralization of PFAS. Further thermodynamic and kinetic studies of gaseous PFAS degradation and the potential to degrade or capture the products of incomplete combustion are warranted.

Formation of CF_4 and C_2F_6 during pyrolysis at high temperatures may be particularly problematic as they are difficult to decompose once formed. One strategy for avoiding their formation may be to conduct pyrolysis below 600 °C, forming olefins or polyfluorinated products that are decomposed more readily in a thermal process with excess O_2. Addition of a Pt catalyst may be beneficial at temperatures below ∼600 °C but does not provide a substantial benefit above 600 °C when oxygen and quartz are present and PFCAs appear to be entirely mineralized.

One mineralized product, SiF_4, appears to be a product of reactions between organofluorine radicals and the quartz reactor, and thus, other coincident materials present in the reactor (e.g., soil silica) should be considered in a computational evaluation of PFAS thermal decomposition. Terminal products such as HF, COF_2, and SiF_4 are likely to be removed well by alkaline scrubbers present in air pollution control devices because they are relatively soluble and hydrolyze under alkaline conditions.

In addition to the implications for thermal treatment, the finding that at lower temperatures with O_2 present, PFCAs can be selectively oxidized to COF_2 on the surface of Pt is valuable in terms of total organofluorine measurements. Organofluorine measurements are currently hampered by interference from inorganic fluorine present in environmental samples. COF_2 is a product that is generated only from combustion of PFASs, cannot be formed from inorganic fluorine (e.g., CaF_2 and NaF), and therefore may be valuable as an organofluorine surrogate, avoiding interference from inorganic fluorine. Selective oxidation of the perfluorocarbon chain $(CF_2)_n$ to COF_2 likely applies to other PFAS species as long as perfluorocarbon radicals or fluorinated olefins are formed during combustion so that COF_2 is subsequently formed through reactions 6−11. In ongoing unpublished work by our team, we have already observed this product from PFOS combustion, and we believe that a COF_2 surrogate measurement of PFASs presents an opportunity for a robust new analytical method.

■ ASSOCIATED CONTENT

Supporting Information

The Supporting Information is available free of charge at https://pubs.acs.org/doi/10.1021/acs.est.2c08210.

Assignment of IR peaks (4400−600 cm^{-1}) recorded during thermal decomposition of PFPrA and PFBA (Table S1), infrared spectra acquired during pyrolysis of PFCAs in N_2 at varying temperatures [(a) PFPrA and (b) PFBA (Figure S1)], infrared spectra of catalyzed pyrolysis products of PFCAs in N_2 at varying temperatures with Pt [(a) PFPrA and (b) PFBA (Figure S2)], infrared spectra acquired during combustion of PFCAs in O_2 at varying temperatures [(a) PFPrA and (b) PFBA (Figure S3)], infrared spectra of catalyzed combustion products of PFCAs in O_2 at varying temperatures with Pt [(a) PFPrA and (b) PFBA (Figure S4)], infrared spectra of products of PFBA at 600 and 780 °C in N_2 (Figure S5), formation of HF during PFPrA and PFBA decomposition at 200 °C (Figure S6), and infrared spectra of products of PFCAs at 300 °C in N_2 and O_2 [(a) PFPrA and (b) PFBA (Figure S7)] (PDF)

■ AUTHOR INFORMATION

Corresponding Author

David Hanigan − *Department of Civil and Environmental Engineering, University of Nevada, Reno, Nevada 89557-0258, United States;* orcid.org/0000-0002-6947-7611; Phone: 775-682-7517; Email: dhanigan@unr.edu

Authors

Junli Wang − *Department of Civil and Environmental Engineering, University of Nevada, Reno, Nevada 89557-0258, United States; Department of Environmental Science, University of California, Riverside, California 92521, United States;* orcid.org/0000-0001-8716-0338

Mingrui Song − *Department of Civil and Environmental Engineering, University of Nevada, Reno, Nevada 89557-0258, United States;* orcid.org/0000-0003-1270-0904

Ibrahim Abusallout − *Fraunhofer USA, Inc., Center Midwest, Division for Coatings and Diamonds Technologies, East Lansing, Michigan 48824, United States; CDM Smith, Boston, Massachusetts 02109, United States; Department of Civil and Environmental Engineering, University of Nevada, Reno, Nevada 89557-0258, United States;* orcid.org/0000-0002-1330-4981

Complete contact information is available at: https://pubs.acs.org/10.1021/acs.est.2c08210

Notes

The authors declare no competing financial interest.

■ ACKNOWLEDGMENTS

This research was supported by the Strategic Environmental Research and Development Program under Grant ER19-1214 and by the National Science Foundation under Grants 2128407 and 2219833. Views, opinions, and/or findings contained in this report are those of the authors and should not be construed as an official Department of Defense position or decision unless so designated by other official documentation.

■ REFERENCES

(1) Whitehead, H. D.; Venier, M.; Wu, Y.; Eastman, E.; Urbanik, S.; Diamond, M. L.; Shalin, A.; Schwartz-Narbonne, H.; Bruton, T. A.; Blum, A.; Wang, Z.; Green, M.; Tighe, M.; Wilkinson, J. T.; McGuinness, S.; Peaslee, G. F. Fluorinated Compounds in North American Cosmetics. *Environmental Science & Technology Letters* **2021**, *8* (7), 538−544.

(2) Schultes, L.; Vestergren, R.; Volkova, K.; Westberg, E.; Jacobson, T.; Benskin, J. P. Per-and polyfluoroalkyl substances and fluorine mass balance in cosmetic products from the Swedish market: implications for environmental emissions and human exposure. *Environmental Science: Processes & Impacts* **2018**, *20* (12), 1680−1690.

(3) Sznajder-Katarzyńska, K.; Surma, M.; Cieślik, I. A Review of Perfluoroalkyl Acids (PFAAs) in terms of sources, applications, human exposure, dietary intake, toxicity, legal regulation, and methods of determination. *J. Chem.* **2019**, *2019*, 2717528.
(4) Abusallout, I.; Holton, C.; Wang, J.; Hanigan, D. Henry's Law constants of 15 per- and polyfluoroalkyl substances determined by static headspace analysis. *Journal of Hazardous Materials Letters* **2022**, *3*, 100070.
(5) Buck, R. C.; Franklin, J.; Berger, U.; Conder, J. M.; Cousins, I. T.; de Voogt, P.; Jensen, A. A.; Kannan, K.; Mabury, S. A.; van Leeuwen, S. P. Perfluoroalkyl and polyfluoroalkyl substances in the environment: terminology, classification, and origins. *Integr Environ. Assess Manag* **2011**, *7* (4), 513−41.
(6) Washington, J. W.; Rankin, K.; Libelo, E. L.; Lynch, D. G.; Cyterski, M. Determining global background soil PFAS loads and the fluorotelomer-based polymer degradation rates that can account for these loads. *Sci. Total Environ.* **2019**, *651* (2), 2444−2449.
(7) Barzen-Hanson, K. A.; Roberts, S. C.; Choyke, S.; Oetjen, K.; McAlees, A.; Riddell, N.; McCrindle, R.; Ferguson, P. L.; Higgins, C. P.; Field, J. A. Discovery of 40 classes of per- and polyfluoroalkyl substances in historical aqueous film-forming foams (AFFFs) and AFFF-impacted groundwater. *Environ. Sci. Technol.* **2017**, *51* (4), 2047−2057.
(8) Brusseau, M. L.; Anderson, R. H.; Guo, B. PFAS concentrations in soils: Background levels versus contaminated sites. *Sci. Total Environ.* **2020**, *740*, 140017.
(9) Lin, H.; Taniyasu, S.; Yamazaki, E.; Wei, S.; Wang, X.; Gai, N.; Kim, J. H.; Eun, H.; Lam, P. K. S.; Yamashita, N. Per- and Polyfluoroalkyl Substances in the Air Particles of Asia: Levels, Seasonality, and Size-Dependent Distribution. *Environ. Sci. Technol.* **2020**, *54* (22), 14182−14191.
(10) Cordner, A.; De La Rosa, V. Y.; Schaider, L. A.; Rudel, R. A.; Richter, L.; Brown, P. Guideline levels for PFOA and PFOS in drinking water: the role of scientific uncertainty, risk assessment decisions, and social factors. *J. Expo Sci. Environ. Epidemiol* **2019**, *29* (2), 157−171.
(11) Huang, K.; Li, Y.; Bu, D.; Fu, J.; Wang, M.; Zhou, W.; Gu, L.; Fu, Y.; Cong, Z.; Hu, B.; Fu, J.; Zhang, A.; Jiang, G. Trophic Magnification of Short-Chain Per- and Polyfluoroalkyl Substances in a Terrestrial Food Chain from the Tibetan Plateau. *Environmental Science & Technology Letters* **2022**, *9* (2), 147−152.
(12) Evich, M. G.; Davis, M. J. B.; McCord, J. P.; Acrey, B.; Awkerman, J. A.; Knappe, D. R. U.; Lindstrom, A. B.; Speth, T. F.; Tebes-Stevens, C.; Strynar, M. J.; Wang, Z.; Weber, E. J.; Henderson, W. M.; Washington, J. W. Per- and polyfluoroalkyl substances in the environment. *Science* **2022**, *375* (6580), No. eabg9065.
(13) Wang, Z.; DeWitt, J. C.; Higgins, C. P.; Cousins, I. T. A Never-Ending Story of Per- and Polyfluoroalkyl Substances (PFASs)? *Environ. Sci. Technol.* **2017**, *51* (5), 2508−2518.
(14) Winchell, L. J.; Ross, J. J.; Wells, M. J. M.; Fonoll, X.; Norton Jr, J. W.; Bell, K. Y. Per- and polyfluoroalkyl substances thermal destruction at water resource recovery facilities: A state of the science review. *Water Environment Research* **2021**, *93* (6), 826−843.
(15) Wang, F.; Lu, X.; Li, X. Y.; Shih, K. Effectiveness and mechanisms of defluorination of perfluorinated alkyl substances by calcium compounds during waste thermal treatment. *Environ. Sci. Technol.* **2015**, *49* (9), 5672−80.
(16) Aleksandrov, K.; Gehrmann, H. J.; Hauser, M.; Matzing, H.; Pigeon, D.; Stapf, D.; Wexler, M. Waste incineration of Polytetrafluoroethylene (PTFE) to evaluate potential formation of per- and Poly-Fluorinated Alkyl Substances (PFAS) in flue gas. *Chemosphere* **2019**, *226*, 898−906.
(17) Duchesne, A. L.; Brown, J. K.; Patch, D. J.; Major, D.; Weber, K. P.; Gerhard, J. I. Remediation of PFAS-Contaminated Soil and Granular Activated Carbon by Smoldering Combustion. *Environ. Sci. Technol.* **2020**, *54* (19), 12631−12640.
(18) Thoma, E. D.; Wright, R. S.; George, I.; Krause, M.; Presezzi, D.; Villa, V.; Preston, W.; Deshmukh, P.; Kauppi, P.; Zemek, P. G. Pyrolysis processing of PFAS-impacted biosolids, a pilot study. *J. Air Waste Manag Assoc* **2022**, *72* (4), 309−318.
(19) Kundu, S.; Patel, S.; Halder, P.; Patel, T.; Hedayati Marzbali, M.; Pramanik, B. K.; Paz-Ferreiro, J.; de Figueiredo, C. C.; Bergmann, D.; Surapaneni, A.; Megharaj, M.; Shah, K. Removal of PFASs from biosolids using a semi-pilot scale pyrolysis reactor and the application of biosolids derived biochar for the removal of PFASs from contaminated water. *Environmental Science: Water Research & Technology* **2021**, *7* (3), 638−649.
(20) Watanabe, N.; Takata, M.; Takemine, S.; Yamamoto, K. Thermal mineralization behavior of PFOA, PFHxA, and PFOS during reactivation of granular activated carbon (GAC) in nitrogen atmosphere. *Environmental Science and Pollution Research* **2018**, *25* (8), 7200−7205.
(21) Xiao, F.; Sasi, P. C.; Yao, B.; Kubátová, A.; Golovko, S. A.; Golovko, M. Y.; Soli, D. Thermal stability and decomposition of perfluoroalkyl substances on spent granular activated carbon. *Environmental Science & Technology Letters* **2020**, *7* (5), 343−350.
(22) Sonmez Baghirzade, B.; Zhang, Y.; Reuther, J. F.; Saleh, N. B.; Venkatesan, A. K.; Apul, O. G. Thermal Regeneration of Spent Granular Activated Carbon Presents an Opportunity to Break the Forever PFAS Cycle. *Environ. Sci. Technol.* **2021**, *55* (9), 5608−5619.
(23) Ge, Y.; Liu, Z.-z.; Liu, H.-x.; Feng, J.-K.; Liu, D.-s.; Ge, X.-w. Theoretical study on the degradation reaction mechanism of elimination hydrogen fluoride from perfluoropropionic acid. *Computational and Theoretical Chemistry* **2014**, *1029*, 33−40.
(24) Altarawneh, M. A theoretical study on the pyrolysis of perfluorobutanoic acid as a model compound for perfluoroalkyl acids. *Tetrahedron Lett.* **2012**, *53* (32), 4070−4073.
(25) Altarawneh, M.; Almatarneh, M. H.; Dlugogorski, B. Z. Thermal decomposition of perfluorinated carboxylic acids: Kinetic model and theoretical requirements for PFAS incineration. *Chemosphere* **2022**, *286* (2), 131685.
(26) Wu, J.; Liu, Z.-z.; Liu, H.-x.; Liu, D.-s.; Ge, X.-w. Theoretical Study on Decomposition Mechanism of Perfluoropentanoic Acid. *Neimenggu Daxue Xuebao, Ziran Kexueban* **2013**, No. 3, 17.
(27) Krusic, P. J.; Marchione, A. A.; Roe, D. C. Gas-phase NMR studies of the thermolysis of perfluorooctanoic acid. *J. Fluorine Chem.* **2005**, *126* (11), 1510−1516.
(28) Stockenhuber, S.; Weber, N.; Dixon, L.; Lucas, J.; Grimison, C.; Bennett, M.; Stockenhuber, M.; Mackie, J.; Kennedy, E. Thermal Degradation of Perfluorooctanoic Acid (PFOA). 16th Internationl Conference on Environmental Science and Technololgy Rhodes, Greece, 2019.
(29) Xiao, F.; Sasi, P. C.; Alinezhad, A.; Golovko, S. A.; Golovko, M. Y.; Spoto, A. Thermal Decomposition of Anionic, Zwitterionic, and Cationic Polyfluoroalkyl Substances in Aqueous Film-Forming Foams. *Environ. Sci. Technol.* **2021**, *55* (14), 9885−9894.
(30) Sasi, P. C.; Alinezhad, A.; Yao, B.; Kubátová, A.; Golovko, S. A.; Golovko, M. Y.; Xiao, F. Effect of Granular Activated Carbon and Other Porous Materials on Thermal Decomposition of Per- and Polyfluoroalkyl Substances: Mechanisms and Implications for Water Purification. *Water Res.* **2021**, *200*, 117271.
(31) Wang, J.; Lin, Z.; He, X.; Song, M.; Westerhoff, P.; Doudrick, K.; Hanigan, D. Critical Review of Thermal Decomposition of Per- and Polyfluoroalkyl Substances: Mechanisms and Implications for Thermal Treatment Processes. *Environ. Sci. Technol.* **2022**, *56* (9), 5355−5370.
(32) Wang, J.; Abusallout, I.; Song, M.; Marfil-Vega, R.; Hanigan, D. Quantification of per- and polyfluoroalkyl substances with a modified total organic carbon analyzer and ion chromatography. *AWWA Water Sci.* **2021**, *3* (4), No. e1235.
(33) Wang, F.; Lu, X.; Shih, K.; Liu, C. Influence of calcium hydroxide on the fate of perfluorooctanesulfonate under thermal conditions. *Journal of Hazardous Materials* **2011**, *192* (3), 1067−71.
(34) Watanabe, N.; Takemine, S.; Yamamoto, K.; Haga, Y.; Takata, M. Residual organic fluorinated compounds from thermal treatment of PFOA, PFHxA and PFOS adsorbed onto granular activated carbon

https://doi.org/10.1021/acs.est.2c08210
Environ. Sci. Technol. 2023, 57, 6179−6187

(GAC). *Journal of Material Cycles and Waste Management* **2016**, *18* (4), 625−630.
(35) D'Ambro, E. L.; Pye, H. O. T.; Bash, J. O.; Bowyer, J.; Allen, C.; Efstathiou, C.; Gilliam, R. C.; Reynolds, L.; Talgo, K.; Murphy, B. N. Characterizing the Air Emissions, Transport, and Deposition of Per- and Polyfluoroalkyl Substances from a Fluoropolymer Manufacturing Facility. *Environ. Sci. Technol.* **2021**, *55* (2), 862−870.
(36) Krug, J. D.; Lemieux, P. M.; Lee, C. W.; Ryan, J. V.; Kariher, P. H.; Shields, E. P.; Wickersham, L. C.; Denison, M. K.; Davis, K. A.; Swensen, D. A.; Burnette, R. P.; Wendt, J. O. L.; Linak, W. P. Combustion of C1 and C2 PFAS: Kinetic modeling and experiments. *J. Air Waste Manag Assoc* **2022**, *72* (3), 256−270.
(37) Aro, R.; Eriksson, U.; Karrman, A.; Reber, I.; Yeung, L. W. Y. Combustion ion chromatography for extractable organofluorine analysis. *iScience* **2021**, *24* (9), 102968.
(38) Bamdad, H.; Papari, S.; Moreside, E.; Berruti, F. High-Temperature Pyrolysis for Elimination of Per- and Polyfluoroalkyl Substances (PFAS) from Biosolids. *Processes* **2022**, *10* (11), 2187.
(39) Linstrom, P. J., Mallard, W. G., Eds. *NIST Chemistry WebBook, NIST Standard Reference Database Number 69*; National Institute of Standards and Technology: Gaithersburg, MD, 20899 DOI: 10.18434/T4D303 (accessed 2022-03-09).
(40) SpectraBase. https://spectrabase.com/ John Wiley & Sons, Inc. (accessed 2022-03-09).
(41) Roehl, C.; Boglu, D.; Brühl, C.; Moortgat, G. Infrared band intensities and global warming potentials of CF4, C2F6, C3F8, C4F10, C5F12, and C6F14. *Geophysical research letters* **1995**, *22* (7), 815−818.
(42) Stepanov, S.; Gabriel, O.; Meichsner, J. In Correlation between CF_2 -and C_2F_4 concentrations in pulsed capacitively coupled CF_4/H_2 rf plasma. *XXVIII International Conference on Phenomena in Ionised Gases (ICPIG 2007)*; July 15−20, 2007, Prague, Czech Republic; Institute of Physics, 2007; pp 1602−1605.
(43) Stevens, J. E.; Macomber, L. D.; Davis, L. W. IR spectra and vibrational modes of the hydrofluoroethers CF3OCH3, CF3OCF2H, and CF3OCF2CF2H and corresponding alkanes CF3CH3, CF3CF2H, and CF3CF2CF2H. *Open Physical Chemistry Journal* **2010**, *4* (1), 17−27.
(44) Center, A. T.; Ground, A. P. Measurement of Carbonyl Fluoride, Hydrogen Fluoride, and Other Combustion Byproducts During Fire Suppression Testing by Fourier Transform Infrared Spectroscopy. Halon Options Technical Working Conference; 1998.
(45) Mashino, M.; Ninomiya, Y.; Kawasaki, M.; Wallington, T. J.; Hurley, M. D. Atmospheric Chemistry of CF3CF = CF2: Kinetics and Mechanism of Its Reactions with OH Radicals, Cl Atoms, and Ozone. *J. Phys. Chem. A* **2000**, *104* (31), 7255−7260.
(46) Liang, J.; Safriet, A.; Briley, S.; Roselius, M. Chemisorption study of trifluoroacetyl fluoride on FeF3 by FT-IR spectroscopy. *J. Fluorine Chem.* **1996**, *79* (1), 53−57.
(47) Mosiadz, M.; Juda, K. L.; Hopkins, S. C.; Soloducho, J.; Glowacki, B. A. An in-depth in situ IR study of the thermal decomposition of yttrium trifluoroacetate hydrate. *J. Therm. Anal. Calorim.* **2012**, *107* (2), 681−691.
(48) Malanca, F. E.; Bierbrauer, K. L.; Chiappero, M. S.; Argüello, G. A. Photochemistry of fluorinated compounds. Kinetics of the reaction between CF_3CF_2 and FCO radicals. *J. Photochem. Photobiol., A* **2002**, *149*, 9.
(49) Jollie, D.; Harrison, P. An in situ IR study of the thermal decomposition of trifluoroacetic acid. *J. Chem. Soc., Perkin Trans.* **1997**, *2* (8), 1571−1576.
(50) Moore, L. O. Pyrolysis of heptafluorobutyric anhydride. *Journal of Organic Chemistry* **1970**, *35* (9), 3201−3202.
(51) Weber, N. H.; Stockenhuber, S. P.; Delva, C. S.; Abu Fara, A.; Grimison, C. C.; Lucas, J. A.; Mackie, J. C.; Stockenhuber, M.; Kennedy, E. M. Kinetics of Decomposition of PFOS Relevant to Thermal Desorption Remediation of Soils. *Ind. Eng. Chem. Res.* **2021**, *60* (25), 9080−9087.
(52) LaZerte, J. D.; Hals, L. J.; Reid, T. S.; Smith, G. H. Pyrolyses of the Salts of the Perfluoro Carboxylic Acids. *J. Am. Chem. Soc.* **1953**, *75* (18), 4525−4528.
(53) Atkinson, B.; Trenwith, A. 424. The thermal decomposition of tetrafluorethylene. *Journal of the Chemical Society (Resumed)* **1953**, 2082−2087.
(54) Atkinson, B.; Atkinson, V. 401. The thermal decomposition of tetrafluoroethylene. *Journal of the Chemical Society (Resumed)* **1957**, 2086−2094.
(55) Butler, J. N. The Thermal Decomposition of Octafluorocyclobutane. *J. Am. Chem. Soc.* **1962**, *84* (8), 1393−1398.
(56) Corbett, P.; Whittle, E. 604. The thermal decomposition of perfluoroacetic anhydride. *Journal of the Chemical Society (Resumed)* **1963**, 3247−3251.
(57) Steunenberg, R. K.; Cady, G. H. Pyrolysis of fluorocarbons1. *J. Am. Chem. Soc.* **1952**, *74* (16), 4165−4168.
(58) Yu, H.; Kennedy, E. M.; Mackie, J. C.; Dlugogorski, B. Z. An Experimental and Kinetic Modeling Study of the Reaction of CHF3 with Methane. *Environ. Sci. Technol.* **2006**, *40* (18), 5778−5785.
(59) Yu, H.; Kennedy, E. M.; Ong, W.-H.; Mackie, J. C.; Han, W.; Dlugogorski, B. Z. Experimental and Kinetic Studies of Gas-phase Pyrolysis of n-C4F10. *Ind. Eng. Chem. Res.* **2008**, *47* (8), 2579−2584.
(60) Donadio, D.; Ghiringhelli, L. M.; Delle Site, L. Autocatalytic and cooperatively stabilized dissociation of water on a stepped platinum surface. *J. Am. Chem. Soc.* **2012**, *134* (46), 19217−22.
(61) van Spronsen, M. A.; Frenken, J. W. M.; Groot, I. M. N. Observing the oxidation of platinum. *Nat. Commun.* **2017**, *8* (1), 429.
(62) Gland, J. L.; Sexton, B. A.; Fisher, G. B. Oxygen interactions with the Pt(111) surface. *Surf. Sci.* **1980**, *95* (2), 587−602.
(63) Wilf, M.; Dawson, P. T. The adsorption and desorption of oxygen on the Pt(110) surface; A thermal desorption and LEED/AES study. *Surf. Sci.* **1977**, *65* (2), 399−418.
(64) Peterson, S. D.; Francisco, J. S. Theoretical study of the thermal decomposition pathways of 2-H heptafluoropropane. *J. Phys. Chem. A* **2002**, *106* (13), 3106−3113.
(65) Palmer, R. L.; Smith Jr, J. N. Molecular beam study of CO oxidation on a (111) platinum surface. *J. Chem. Phys.* **1974**, *60* (4), 1453−1463.
(66) Altarawneh, M.; Almatarneh, M. H.; Dlugogorski, B. Z. Thermal decomposition of perfluorinated carboxylic acids: Kinetic model and theoretical requirements for PFAS incineration. *Chemosphere* **2022**, *286*, 131685.
(67) Wang, J.; Lin, Z.; He, X.; Song, M.; Westerhoff, P.; Doudrick, K.; Hanigan, D. Critical Review of Thermal Decomposition of Per- and Polyfluoroalkyl Substances: Mechanisms and Implications for Thermal Treatment Processes. *Environ. Sci. Technol.* **2022**, *56* (9), 5355−5370.
(68) Crownover, E.; Oberle, D.; Kluger, M.; Heron, G. Perfluoroalkyl and polyfluoroalkyl substances thermal desorption evaluation. *Remediation Journal* **2019**, *29* (4), 77−81.
(69) Sorengard, M.; Lindh, A. S.; Ahrens, L. Thermal desorption as a high removal remediation technique for soils contaminated with per- and polyfluoroalkyl substances (PFASs). *PLoS One* **2020**, *15* (6), No. e0234476.

https://doi.org/10.1021/acs.est.2c08210
Environ. Sci. Technol. 2023, 57, 6179−6187